

Convex Models for Optimal Utility Based Distributed Generation Allocation in Radial Distribution Systems

Mohammad Amin Akbari, Jamshid Aghaei, *Senior Member, IEEE*, Mostafa Barani, *Student Member, IEEE*, Taher Niknam, Sahand Ghavidel, *Student Member, IEEE*, Hossein Farahmand, Magnus Korpas, and Li Li, *Member, IEEE*

Abstract—this paper introduces various models for optimal and maximal utility-based distributed generation penetration in the radial distribution systems. Several problems with different probabilistic indices as objective functions constrained by power flow equations, distributed generation penetration, voltage, and thermal limits are proposed to obtain the optimal penetration of distributed generations on rural distribution networks. There are trade-offs between interests and risks that the distribution network operators or distribution companies may be willing to take on. Thus, to have effective method for maximal allocation of distributed generations, new indices are proposed and the problems are formulated as a risk-constrained optimization model. The obtained problems have mixed integer non-linear programming and nonconvex forms because of nonlinearity and nonconvexity of the optimal power flow (OPF) equations and indices, leading to computationally NP-hard problems. Accordingly, in this paper, convex relaxations of OPF are introduced instead of the conventional nonlinear equations. Efficient linear equivalents of the objective function and constraints are introduced to reduce the computational burden. Test results of the proposed models on a radial distribution system are presented and discussed.

Index Terms—Distributed generation, voltage profile, energy losses, risk constraints, convex models, mixed integer programming, quadratic programming.

NOMENCLATURE

A. Indices and Sets

\mathcal{E}	Set of all lines.
\mathcal{G}	Set of generator buses.
h (\mathcal{H})	Index (set) for hours.
i, j, k (\mathcal{N})	Index (set) for buses.
s (\mathcal{S})	Index (set) for scenarios.
t (\mathcal{T})	Index (set) for days.

B. Constants

C_W	Capacity factor of the available wind turbine.
C_S	Capacity factor of the available PV module.
EL^0	Energy losses in the base case.
F	Feeder capacity.
$\gamma_i(t, h)$	The importance factor of bus i .
H	Number of hours.
$l_{max,ij}$	Square value of the ampacity of line ij .
$LC_{max,ij}$	Maximum capacity of line ij .
$LL_{ij}^0(t, h)$	Line-loss in the base case.

M. A. Akbari, J. Aghaei, M. Barani and T. Niknam are with the Department of Electrical and Electronics Engineering, Shiraz University of Technology, Shiraz, Iran (e-mails: m.akbari@sutech.ac.ir; aghaei@sutech.ac.ir; m.barani@sutech.ac.ir).

S. Ghavidel and L. Li are with Faculty of Engineering and Information Technology, University of Technology, Sydney, PO Box 123, Broadway, NSW 2007, Australia (e-mails: sahand.ghavidel@jirsaraie@student.uts.edu.au; li.li@uts.edu.au).

H. Farahmand and M. Korpas are with Department of Electric Power Engineering, Norwegian University of Science and Technology (NTNU), Trondheim NO-7491, Norway (e-mails: hossein.farahmand@ntnu.no; magnus.korpas@ntnu.no).

λ	Maximum penetration limit in the system.
M	Big value for the linearization.
N	Number of buses.
$Ntap$	Number of tap positions.
$P_{bus,i}$	Maximum allowable penetration in bus i .
$P_{D,i}^s(t, h)$	Active power of the load connected to bus i .
P_W^r	Rated capacity of wind turbine.
P_S^r	Rated capacity of PV module.
P_B^r	Rated capacity of biomass DG unit.
$P_W^s(t, h)$	Output power of wind turbine.
$P_S^s(t, h)$	Output power of PV module.
$Q_{D,i}^s(t, h)$	Reactive power of the load connected to bus i .
r_{ij}	Resistance of line ij .
ρ_s	Probability of scenario s .
T	Number of days.
T_{min}	Minimum voltage magnitude at the lowest tap position.
T_{tap}	Step ratiot.
$v_{min,i}$	Lower limit of voltage in bus i .
$v_{max,i}$	Upper limit of voltage in bus i .
$v_i^0(t, h)$	Square of voltage magnitude in bus i in the base case.
x_{ij}	Reactance of line ij .
z_{ij}	Impedance of line ij .

C. Variables

$BIVR_i^s(t, h)$	Binary value for indicating interest voltage rise states in bus i .
$BLFO_{ij}^s(t, h)$	Binary value for indicating line-flow overloading states in line ij .
$BLLI_{ij}^s(t, h)$	Binary value for indicating line-loss increment states in line ij .
$BLLR_{ij}^s(t, h)$	Binary value for indicating line-loss reduction states in line ij .
$BRVD_i^s(t, h)$	Binary value for indicating risky voltage down states in bus i .
$BRVR_i^s(t, h)$	Binary value for indicating risky voltage rise states in bus i .
$\eta_n^s(t, h)$	Binary variable for counting OLTC tap ratios.
EL	Energy losses after DG integration.
ELI	Energy losses index.
$ELLI$	Expected line-loss increment.
$ELLR$	Expected line-loss reduction.
$IVRP$	Interest voltage rise probability.
$l_{ij}^s(t, h)$	The square of the magnitude of current from bus i to bus j .
$LFOP$	Line-flow overloading probability.
$LI_{ij}^s(t, h)$	The amount of line-loss increment.

$LR_{ij}^s(t, h)$	The amount of line-loss reduction.
$LL_{ij}^s(t, h)$	Line-loss after DG integration.
$n_{B,i}$	Integer value of biomass DG units to be installed in bus i .
$n_{S,i}$	Integer value of the PV modules to be installed in bus i .
$n_{W,i}$	Integer value of the wind turbines to be installed in bus i .
$P_{B,i}$	Capacity of biomass DG unit to be installed in bus i .
$P_{DG,i}^s(t, h)$	DG power generation in bus i .
$P_{ij}^s(t, h)$	Sending-end active power flow from bus i to bus j .
$P_{S,i}$	Capacity of the PV module to be installed in bus i .
$P_{W,i}$	Capacity of the wind turbine to be installed in bus i .
$Q_{ij}^s(t, h)$	Sending-end reactive power flow from bus i to bus j .
RVP	Risky voltage probability.
$v_i^s(t, h)$	The square of the magnitude of voltage in bus i .
VI	Voltage stability index.

I. INTRODUCTION

DISTRIBUTED generation (DG) has rapidly increased in recent years. Introduction of DGs changes the magnitude and even the direction of power flows. This may be interesting (if optimally allocated) from many points of view, but for a higher levels of penetration (or inappropriate placement) it may raise several potential operation challenges. Therefore, distribution system (DS) operation and planning practices of distribution companies (DISCOs) are affected by integrating DG from both technical and economic implications points of view. For example, from supply security perspective, employment of DGs needs revising the design and coordination of protective devices; from the DS operation perspective, voltage profiles, energy losses, and maintenance and system restoration practices (in the case of faults) are also affected; and finally from DS design and planning perspective, grid reinforcement and additions should take into account future DG connections. It is also true that more renewable DGs are needed to achieve environmental targets. Therefore, new techniques are needed to determine the optimal and maximal allocation of DGs in the existing DS for improving its performance. Hence, optimal and maximal allocation of DGs in the distribution system is one of the most crucial issues of DG planning.

Because of non-linearity associated with the objective functions, technical constrains and AC power flow equations as well as discrete nature of the DG size and location, optimal DG allocation (ODGA) belongs to a family of optimization known as the mixed integer nonlinear programming (MINLP) problems. Furthermore, it will become more complex when counting time-varying characteristics of the loads and DGs' output power. Therefore, robust methods are needed to solve such a nondeterministic polynomial-time hard (NP-hard) problem in an effective way.

The promise of effective ODGA in the DS is widely accepted and has led to a great deal of research activities [1]–[33]. A brief overview of some of the recent works is given in Table I. From the current literature, the methods of solving ODGA problem can be

classified into analytical [1]–[7], numerical [8]–[25] and population-based [26]–[33] methods. Analytical methods are straightforward alternatives to find the optimum size and location of DGs for a specific technical performance over a simplified cluster of relations and iterations and they are computationally fast. Two analytical methods are presented in [1] for finding optimal location of a single DG with fixed size in the radial and meshed networks. Another analytical method is introduced in [2] which uses a loss sensitivity analysis to get the optimum size and site of a single DG. Authors in [3] propose analytical expressions for the optimal placement of one and two DGs. An analytical method as well as Kalman filter algorithm are investigated in [4] for finding the optimal location and size of multiple DGs. Authors in [5] suggest analytical expressions for finding optimal size and power factor of different types of DGs. Problem of multiple distributed generators (DG units) placement to achieve a high loss reduction in large-scale primary distribution networks is investigated in [6]. In [7], the combination of analytical and genetic algorithm methods is used for an optimal allocation of multiple DGs in a distribution network to minimize the system losses. The main disadvantages of this class of approaches are: a) traditionally, a single peak load scenario is considered to calculate the power losses rather than energy losses, while load demand and DG's output power have time-varying nature and also distribution network operator (DNO) and DISCOs use energy losses measure; b) as the analytical formulation is only provided for a single technical attribute, accordingly different potential limitations such as voltage down/rise and line overloading as well as voltage control schemes have not been considered; c) for a given time period, only one DG plant can be assessed, i.e., an iterative procedure is required for multiple connections of DGs. Thus, these methods result in only declarative solutions.

Numerical methods have been widely used and developed for solving ODGA problem. Gradient search and sequential quadratic programming are used to solve ODGA constrained by fault levels in [8], [9], respectively. Authors in [10] utilize linear programming to solve the problem of ODGA in order to maximize the DG energy harvesting. ODGA problem is formulated as the nonlinear programming in [11]–[13]. MINLP is employed for optimal allocation of different types of DG units in the hybrid electricity market in [14] and the electricity market price fluctuation has been considered in [15]. Authors in [16] and [17] introduce probabilistic-based MINLP models for the energy losses minimization by the allocation of only wind power generation and mix of renewable DGs, respectively. The same model for the placement of DGs for the voltage stability improvement is introduced in [18]. Authors in [19] utilize a dynamic programming model to solve the problem of the optimal placement of DGs in a distribution system with the objectives of power loss minimization, voltage profile improvements and reliability maximization. An ordinal optimization method is proposed in [20] for exploring the trade-offs between the loss minimization and DG penetration maximization. Exhaustive searches are proposed for solving the ODGA in distribution networks with different load models in [21], with time-varying generation and load model in [22], and through the evaluation of interests and risks analysis using several performance-based metrics in [23]. A stochastic-based mixed-integer conic programming (MICP) formulation for optimal wind generation allocation is presented in [24], [25] with the objective of maximizing a multiobjective performance index.

As mentioned, the ODGA problem belongs to the MINLP problems which are well-known for their complexity and computationally expensive features. Due to the lack of efficient mathematical approaches for solving this class of optimization problems within a reasonable time, the heuristic algorithms have been widely used in the literature to find fast, while suboptimal solutions. There are many heuristic methods that have been applied to the problem of ODGA with different characteristics. For example, genetic algorithm (GA) is used in [26] to solve single and multiobjective models of ODGA. Authors in [27] use GA combined with Tabu search (TS) to solve a stochastic planning model to minimize the life-cycle cost of the DG constrained by the reliability criterion. Particle swarm optimization (PSO) is implemented in [28] for maximizing DG penetration with the harmonic and protection constraints. Ant colony optimization (ACO) is proposed in [29] for co-optimal placement of protection devices and DGs for reliability enhancement in radial distribution networks. Artificial bee colony (ABC) is presented in [30] for determining optimum size, power factor, and location with the objective of power losses minimization. In [31] differential evolution (DE) algorithm is proposed for minimizing transmission losses by optimally allocating DGs in a sub-transmission system. Harmony search (HS) is presented in [32] to solve the problem of network reconfiguration in the presence of DGs in order to minimize the real power losses and improve the voltage profile in a distribution system. Practical heuristic algorithms (PHA) is proposed in [33] for ODGA in a distribution system with the objective of reliability improvement. Despite their broad applicabilities, the intrinsic problem structure which is important for the large-scale problems, is often neglected in the heuristic methods [34]. The intrinsic structure of a problem includes linearity, convexity, differentiability, and continuity of the objective function and constraints. The heuristic methods such as GA, SA, PSO, TS, and etc., consider the problem as a “black box” and hence, they may neglect the intrinsic problem structure. In addition, these population approaches have no guarantee for finding optimal solutions within a finite amount of time, parameter tuning mostly is done by the trial-and-error strategy, they may be expensive and have no complete theoretical basis yet [34], [35].

Due to the nonconvexity of the power flow equations and some constraints, most problems of ODGA are nonconvex; resulting in no assurance of convergence to the global solution. Recent researches have shown that the load flow equations describing the steady-state conditions in the distribution network can be placed in the extended conic quadratic format [24], [25], [34]–[37]. The implementation of this format in the OPF problem is proposed in [38] considering several control devices such as tap-changing transformers, phase-shifting transformers, and unified power flow controllers. Authors in [34], [35], [39] propose MICP formulation for the minimum loss distribution network reconfiguration problem based on the recently developed convex relaxation of the AC OPF problem. Reference [34] has the extended convex relaxations of the network reconfiguration problem which is differ from the ODGA problem as each problem has its own mathematical format.

In summery, to the best of authors’ knowledge, the contributions of this paper with respect to the researches in the area are: (i) The uncertain characteristics of renewable DG units and loads for ODGA are taken into account in the distribution systems towards higher performance networks. (ii) New performance-based indices have been introduced and formulated which comprehensively evaluate the

TABLE I
TAXONOMY OF THE REVIEWED ODGA MODELS.

Technique	Analytical	[1]–[7]
	Numerical	[8]–[25]
	Heuristic	[26]–[33].
Objective	Single objective	[1]–[10], [13], [14], [16]–[18], [21], [42]–[44]
	Multi objective	[12], [15], [22]–[25]
Objective function	Min power loss	[1]–[7], [9], [21]
	Min energy loss	[16], [17], [23]–[25], [44]
	Max profit	[10], [19], [20], [43]
	Min cost	[14], [42]
	Max voltage	[18], [23], [24]
	Max penetration	[8], [13], [25], [45]
Design variable	Type	[17], [18], [23]–[25]
	Size	[2]–[9], [13]–[21], [23]–[25], [42]–[45]
	Site	[1]–[8], [10], [12], [14]–[21], [23]–[25], [42]–[45]
	Number	[14], [17], [18]
OPF	Linear/ Convex	[8], [24], [25]
	Non-linear/Nonconvex	[9], [10], [14]–[18], [20], [21], [45]
Modeling	Deterministic	[1]–[10], [20], [21], [42]
	Stochastic	[12], [16]–[18], [22]–[25], [43], [45]

steady state technical impacts of DGs’ penetration on the distribution networks. These indices include both interests and risks of DGs’ penetration. (iii) A basic probabilistic-based AC OPF technique is provided to minimize energy losses, maximize voltage profile and find maximal DGs’ penetration by optimally allocating DGs in the distribution systems. (iv) Mixed-integer quadratic programming (MIQP), mixed-integer quadratically constrained programming (MIQCP), and second-order cone programming (MISOCP) formulations are extracted for ODGA, as seen in Table II. Furthermore, efficient linearization and relaxation techniques are used to exploit these models which can be solved using available powerful commercial softwares. (v) Risk-based maximal DG penetration in the distribution systems is formulated and evaluated using MIQCP model considering the probability of voltage constraint violation and line flow overloading as the risk constraints. (vi) The potential advantages of adopting real-time control and communication systems as a part of the future smart grids are evaluated in the problems of ODGA.

The main advantage of the above-mentioned features in the proposed models is that the ODGA problem can be solved using available powerful commercial software such as CPLEX [40] and GUROBI [41]. Also, unlike the most population-based optimization algorithms, the proposed models guarantee the optimal global solution. The rest of the paper is organized as follows: In Section II, the model description of renewable energy resources and load is presented. The problem formulation of ODGA is reviewed in Section III. The proposed convex relaxations of the obtained nonconvex formulation are explained in Section IV. Section V proposes additional interests and risks of implementing DGs. The results obtained by applying the proposed models to a variety of case studies are demonstrated in Section VI. The conclusions are summarized in Section VII.

II. MODEL DESCRIPTION

A. Modeling of Renewable Resources

1) *Data*: In this paper, the probabilistic generation of each DG unit has been modeled according to the hourly historical data of the site under study, during two years, as well as specific characteristics of each DG. On this basis, each year is divided into four seasons. In order to characterize the random behavior of the renewable energy resources during each season, a typical day with 24-h time periods is considered. For each season, the data related to the same hours of the day are utilized to obtain the probability distribution functions (PDFs) corresponding to each time period. The probabilistic model of DGs including wind turbines (WTs) and PV systems are characterized as follows.

2) *Probabilistic Model of WTs and PV System*: The hourly wind speed and solar irradiance of the site under study have been utilized to generate Rayleigh [46] and Beta [47] distribution functions for each time period, respectively. These continuous PDFs are sliced into several segments where each segment yields a mean value and a probability of occurrence. Note that the probability of each segment during any specific hour can be expressed as follows:

$$\text{prob}_i = \int_{X_i}^{X_{i+1}} f(x) dx \quad (1)$$

where $f(x)$ indicates PDFs. X_i and X_{i+1} are the starting and ending points of the interval i , respectively.

B. Load Data

From the hourly load data for the system under study and the IEEE-RTS system [48], the load profile is considered as a percentage of the annual peak load.

C. Whole System Characterization

- *Generating related PDFs*: Firstly, the PDFs for solar irradiance and wind speed are obtained using historical data (24 PDFs for each season related to 24-h of a typical day). As it was discussed in the previous section, these continuous PDFs are sliced into several segments for each time period.
- *Developing scenarios with their own probability*: Next, the different realization of the random variables, i.e., solar irradiance and wind speed are generated using the roulette wheel mechanism [46], separately. By the way of illustration, consider winter which is modeled through a typical day with a 24-h time period. In this case, N_S and N_W scenarios are generated for solar irradiance and wind speed, respectively. For example, for solar irradiance, each scenario contains 24 values of solar irradiance related to the 24-h time period of the typical day. It should be noted that each scenario has its own probability of occurrence.
- *calculating the output power of DGs*: Then, based on the characteristics and power curves of DG units, the solar irradiance and wind speed of each state during each time period is transformed into the output power of PV and wind-based units.
- *Reducing the number of scenarios*: A large number of scenarios may contribute to a more accurate model of the random variables. Nevertheless, this increases the computational burden

of the problem. Thus, finally, a fast forward scenario reduction method based on the Kontorwisch distance [49] is employed to reduce the number of scenarios while provides a reasonable approximation of random variable of the system.

For more details about the probabilistic modeling the work [23] is suggested.

III. ODGA PROBLEM FORMULATION

A. Notations

A radial distribution system (RDS) can be represented by the graph $G = (\mathcal{N}, \mathcal{E})$ and the set of generator buses $\mathcal{G} \subseteq \mathcal{N}$. Let $\mathcal{N} := \{1, \dots, n\}$ denote the collection of all nodes. Each line connects an ordered pair (i, j) of nodes where node i is the sending end and node j is the receiving end bus. Let \mathcal{E} denote the collection of all lines, and $(i, j) \in \mathcal{E}$ is abbreviated by ij for convenience. Note that, as G is directed, if $(i, j) \in \mathcal{E}$ then, $(j, i) \notin \mathcal{E}$. For each bus $i \in \mathcal{N}$, let $V_i^s(t, h) = V_{re,i}^s(t, h) + \mathbf{i}V_{im,i}^s(t, h)$ denote its complex voltage and it is defined that $v_i^s(t, h) := |V_i^s(t, h)|^2$. Let $I_{ij}^s(t, h) = I_{re,ij}^s(t, h) + \mathbf{i}I_{im,ij}^s(t, h)$ denote the complex current from bus i to bus j and it is defined that $l_{ij}^s(t, h) := |I_{ij}^s(t, h)|^2$.

B. Constraints

1) *Power Flow Equations*: Given the network graph $(\mathcal{N}, \mathcal{E})$, the impedance z , and the substation voltage v_1 , then the other decision variables satisfy the *DistFow* equations [24]: $\forall (i, j) \in \mathcal{E}, \forall j \in \mathcal{N}, \forall s \in \mathcal{S}, \forall t \in \mathcal{T}$ and $\forall h \in \mathcal{H}$,

$$P_{ij}^s(t, h) - r_{ij}l_{ij}^s(t, h) = -P_{DG,j}^s(t, h) + P_{D,j}^s(t, h) + \sum_{k:j \rightarrow k} P_{jk}^s(t, h) \quad (2)$$

$$Q_{ij}^s(t, h) - x_{ij}l_{ij}^s(t, h) = Q_{D,j}^s(t, h) + \sum_{k:j \rightarrow k} Q_{jk}^s(t, h) \quad (3)$$

$$v_i^s(t, h) - v_j^s(t, h) = 2 [r_{ij}P_{ij}^s(t, h) + x_{ij}Q_{ij}^s(t, h)] - |z_{ij}|^2 l_{ij}^s(t, h). \quad (4)$$

2) *Branch Current Equation*: The line current through ij can be expressed as follows: $\forall i \in \mathcal{N}, \forall s \in \mathcal{S}, \forall t \in \mathcal{T}$ and $\forall h \in \mathcal{H}$,

$$l_{ij}^s(t, h) = \frac{P_{ij}^s(t, h)^2 + Q_{ij}^s(t, h)^2}{v_i^s(t, h)}. \quad (5)$$

3) *Voltage Limits*: Bus 1 is reserved for the so-called *slack bus*, which balances the active and reactive power in the system, and it is modeled as a generator: $\forall s \in \mathcal{S}, \forall t \in \mathcal{T}$ and $\forall h \in \mathcal{H}$,

$$v_1^s(t, h) = 1.03 \text{ pu} \quad (6)$$

at the other buses voltage magnitude should lie within pre-specified voltage lower and upper bounds: $\forall i \in \mathcal{N}/\{1\}, \forall s \in \mathcal{S}, \forall t \in \mathcal{T}$ and $\forall h \in \mathcal{H}$,

$$v_{min,i} \leq v_i^s(t, h) \leq v_{max,i}. \quad (7)$$

4) *Feeder Capacity Limits*: Thermal limit of the lines is generally assumed stiff and no overloading is permitted. Accordingly, the maximum thermal capacity of lines should be limited as follows: $\forall (i, j) \in \mathcal{E}, \forall s \in \mathcal{S}, \forall t \in \mathcal{T}$ and $\forall h \in \mathcal{H}$,

TABLE II
ODGA PROBLEMS: OBJECTIVES AND CONSTRAINTS.

Model	MINLP	MIQP	MIQCP	MISOCP
Minimize ELI				
Subject to	(2)-(14)	(9)- (14),(19)- (22)	(6),(7),(9)- (14),(19),(22)- (25)	(2)-(4),(6)- (14),(18)
Maximize VI				
Subject to	(2)-(14)	(6),(7),(9)- (14),(20)- (22),(25)	(6),(7),(9)- (14),(22)- (25)	(2)-(4),(6)- (14),(18)

$$l_{ij}^s(t, h) \leq l_{max,ij}. \quad (8)$$

5) *DG Installed Capacity*: DG installed capacity is equal to the product of selected number of DG units with their rated capacities as follows: $\forall i \in \mathcal{G}$,

$$P_{W,i} = n_{W,i} P_{W,i}^r \quad (9)$$

$$P_{S,i} = n_{S,i} P_S^r \quad (10)$$

$$P_{B,i} = n_{B,i} P_B^r \quad (11)$$

Equations (9)-(11) show sizes of wind turbine, PV and biomass DG units, respectively, which can be installed on each bus in the system.

Aggregation of installed DG capacities on each bus gives: $\forall i \in \mathcal{G}$, $\forall s \in \mathcal{S}$, $\forall t \in \mathcal{T}$ and $\forall h \in \mathcal{H}$,

$$P_{DG,i}^s(t, h) = P_W^s(t, h) P_{W,i} + P_S^s(t, h) P_{S,i} + P_{B,i} \quad (12)$$

where $P_W^s(t, h)$ and $P_S^s(t, h)$ are the output power of wind and PV DGs in scenario s at day t at hour h , respectively as described in section II.

6) *Maximum DG Penetration Limits on Each Bus*: The maximum DG penetration on each bus can be selected according to some factors such as investor decisions, availability of energy resources, land space, etc. The sum of installed ratings of DGs on each bus is limited by the maximum allowable penetration on each bus, $P_{bus,i}$: $\forall i \in \mathcal{G}$,

$$P_{W,i} + P_{S,i} + P_{B,i} \leq P_{bus,i}. \quad (13)$$

7) *Maximum DG Penetration Limits in the System*: Some distribution system companies may have limitations on the percentage of DGs allowed in their systems. The amount of DG power (capacity factor \times DG installed capacity) injected into the network should be restricted by the maximum feeder capacity, F , as follows:

$$\sum_{i \in \mathcal{G}} (C_W P_{W,i} + C_S P_{S,i} + P_{B,i}) \leq \lambda F. \quad (14)$$

C. Objective Functions

From the available literature, two general indices have been used as the objective functions of optimal DG allocation in distribution systems. By comparing and taking the ratio of a measure of an attribute with and without DG (with the same load pattern), an index can be derived for the loss reduction and the voltage profile improvement. The snapshot indices have been proposed in [50]. These indices have been improved and utilized for evaluating DG increasing penetration effects and optimal DG allocation considering the uncertainty of DG and loads in [23] and [24].

We consider the energy loss index and voltage improvement index as objective functions. Thus, a beneficial DG location would decrease total network losses and improve voltage profile. These two indices are defined as the following forms:

1) *Energy Loss Index*: This index should be minimized over a considered time horizon. Since each time segment t represents 90-day (30 days per month \times 3 months per season), this index can be formulated as follows:

$$ELI = \frac{EL}{EL^0} \quad (15)$$

where

$$EL = \sum_{s \in \mathcal{S}} \rho_s \sum_{(i,j) \in \mathcal{E}} \sum_{t \in \mathcal{T}} \sum_{h \in \mathcal{H}} r_{ij} l_{ij}^s(t, h) \times 90 \quad (16)$$

here, ρ_s is the probability of state s . EL and EL^0 denote the energy losses after and before DG addition in the system, respectively.

2) *Voltage Profile Index*: This index can be defined as follows:

$$VI = \frac{1}{T \times H} \sum_{s \in \mathcal{S}} \rho_s \sum_{i \in \mathcal{N}} \sum_{t \in \mathcal{T}} \sum_{h \in \mathcal{H}} \gamma_i(t, h) \left(\frac{v_i^s(t, h)}{v_i^0(t, h)} \right) \quad (17)$$

$v_i^0(t, h)$ is the square of the magnitude of the complex voltage at bus i at time t at hour h in the base case (without DG). T is the total number of time periods during the planning time horizon and H is the total number of hours in a day. $\gamma_i(t, h)$ is the importance factor of load buses which can be chosen based on the importance and criticality of the loads [23], [24]. For the sake of simplicity, all load buses are equally weighted in this paper, i.e., $\gamma_i(t, h) = \frac{1}{N}$; $\forall i \in \mathcal{N}$, $\forall t \in \mathcal{T}$, $\forall h \in \mathcal{H}$; here N is the total number of load buses in the system.

It should be noted that the technical impact indices ELI and VI illustrate that the employment of DG is beneficial or not. If the introduction of DG is beneficial, ELI will be less than unity and VI will be greater than unity. The problem of ODGA tries to find minimum energy loss index (15) and/or maximum voltage improvement index (17) subject to the constraints (2)-(14). The resultant problems has the form of MINLP form.

IV. CONVEX RELAXATIONS OF ODGA

As seen from the above formulations, nonlinear term is only appeared in the equality constraint (5) of the *DistFlow* equations. So, the problem is nonconvex and existing solution methods do not guarantee to find the global solution in a reasonable time [34], [35]. Recently, to cope with these challenges, convex relaxation methods have been proposed and extended by the researchers for the network reconfiguration practices [34], [35], [39]. Convex functions are always somewhat bowl-shaped, have no local maxima (unless constant), and have no more than one local minimum value. If a local minimum exists, then it is also the global minimum. Hence, the gradient descent and Newton methods (with line search) guarantee to produce the global minimum when applied to such functions [51]. The convex forms of the ODGA are extracted below:

A. MISOCP model

As mentioned, the equation of line currents in (5) is nonconvex. If we relax it by the inequality (18) over all lines, we can obtain the MISOCP model of the ODGA problem [24], [52].

$$l_{ij}^s(t, h) \geq \frac{P_{ij}^s(t, h)^2 + Q_{ij}^s(t, h)^2}{v_i^s(t, h)}. \quad (18)$$

This relaxed inequality introduces the second-order cones with respect to (P, Q, l, v) .

B. MIQP Model

Neglecting the l terms in (2)-(4), removing constraints (5)-(7) and fixing the voltage magnitudes at each bus at 1 p.u., the first MIQP formulation of ODGA for energy loss minimization can be obtained. The objective is as (15), and we should only substitute the following quadratic term in (16): $\forall (i, j) \in \mathcal{E}, \forall j \in \mathcal{N}, \forall s \in \mathcal{S}, \forall t \in \mathcal{T}$ and $\forall h \in \mathcal{H}$,

$$l_{ij}^s(t, h) = P_{ij}^s(t, h)^2 + Q_{ij}^s(t, h)^2 \quad (19)$$

and the constraints are (9)-(14) and the linear *DistFlow* equations (20) and (21):

$$P_{ij}^s(t, h) = -P_{DG,j}^s(t, h) + P_{D,j}^s(t, h) + \sum_{k:j \rightarrow k} P_{jk}^s(t, h) \quad (20)$$

$$Q_{ij}^s(t, h) = Q_{D,j}^s(t, h) + \sum_{k:j \rightarrow k} Q_{jk}^s(t, h) \quad (21)$$

C. MIQCP Model

If we reformulate the problem as MIQCP [53], we can write line capacity limit (8) as follows: $\forall (i, j) \in \mathcal{E}, \forall j \in \mathcal{N}, \forall s \in \mathcal{S}, \forall t \in \mathcal{T}$ and $\forall h \in \mathcal{H}$,

$$P_{ij}^s(t, h)^2 + Q_{ij}^s(t, h)^2 \leq LC_{max,ij}^2 \quad (22)$$

Also, the line flow equations (2) and (3) can be replaced by the following quadratic constraints:

$$P_{ij}^s(t, h) - r_{ij} \left(P_{ij}^s(t, h)^2 + Q_{ij}^s(t, h)^2 \right) + P_{DG,j}^s(t, h) - P_{D,j}^s(t, h) - \sum_{k:j \rightarrow k} P_{jk}^s(t, h) \geq 0 \quad (23)$$

$$Q_{ij}^s(t, h) - x_{ij} \left(P_{ij}^s(t, h)^2 + Q_{ij}^s(t, h)^2 \right) - Q_{D,j}^s(t, h) - \sum_{k:j \rightarrow k} Q_{jk}^s(t, h) \geq 0 \quad (24)$$

Furthermore, by removing the last term in (4), this equation can be approximated with the following equality constraint:

$$v_i^s(t, h) - v_j^s(t, h) = 2 \left[r_{ij} P_{ij}^s(t, h) + x_{ij} Q_{ij}^s(t, h) \right]. \quad (25)$$

Accordingly, the MIQCP formulations of ODGA are as given in Table II.

V. PROPOSED NET INTEREST AND RISK INDICES

By comparing a measure of an attribute with and without DG (with the same load pattern), an index can be derived for each attribute. A set of typical indices which can be employed to describe the technical impacts of DG on the DS are: *IVRP*, *RVP*, *LFOP*, *ELLR*, and *ELLI* which have been defined in [23] and mathematically are described below.

A. Interest Voltage Rise Probability (IVRP)

Introducing DG can improve the voltage profile of the system because loads will be served locally resulting in less current flow through the feeder. This reduces the amount of voltage drop and it results in an overall increase of the voltage in the RDS. With the optimal penetration of DG units, the rise in voltage is interesting in the most cases, while improving the voltage profile. For larger amounts of DGs, the effect is more severe for smaller-size feeders, for low-load situations, and for DG units far away from the main substation. In these conditions, the connection of a DG will result in voltages rise above the allowable limit for end-users. The under-voltage is formed by the DG units with induction machine interface where the reactive power consumption could actually result in a reduction of the voltage.

The voltage limit at each node is assessed probabilistically. If the voltage magnitude with DG integration at node i at hour t and state s lays between the lower and upper limits as in (7), and greater than the voltage before adding DG, the voltage rise will be of an interest. In some states, the voltage magnitude may be greater than that of before DG integration, but, still be lower than the minimum voltage limit. These states, however, show the improvement in the voltage profile of the system by DG, which we don't consider as an interest voltage rise, in this paper. A binary variable $BIVR_i^s(t, h)$ is used to count the interest voltage rise. So, $BIVR_i^s(t, h) = 1$, if the voltage of node i in the state s at the day t and at the hour h satisfies (7) and when it is greater than the voltage magnitude without DG employment, it will be equal to zero. As (7) is satisfied in the optimization problem, only condition to count the interest voltage rise is as follows:

$$BIVR_i^s(t, h) = \begin{cases} 1 & ; \text{if } v_i^s(t, h) \geq v_i^0(t, h) \\ 0 & ; \text{otherwise} \end{cases} \quad (26)$$

Let name the probability of these conditions occurring as *IVRP*. The proposed *IVRP* quantifies the improvement in the voltage profile in a simple manner in the presence of DG. Mathematically, it is defined as follows:

$$IVRP = \frac{1}{T \times H} \sum_{s \in \mathcal{S}} \rho_s \sum_{i \in \mathcal{N}} \sum_{t \in \mathcal{T}} \sum_{h \in \mathcal{H}} \gamma_i(t, h) BIVR_i^s(t, h) \quad (27a)$$

$$v_i^s(t, h) - v_i^0(t, h) > [BIVR_i^s(t, h) - 1] M \quad (27b)$$

$$v_i^s(t, h) - v_i^0(t, h) < BIVR_i^s(t, h) M \quad (27c)$$

Also, considering the duration of each time period in (8) we can obtain the duration of the interest voltage rise as another voltage performance metric, if needed.

B. Risky Voltage Probability (RVP) and Line Flow Overloading Probability (LFOP)

If in the OPF it is allowed that voltage constraints can be violated as in BS EN50160 standard [54], and power flows through lines or transformers are also allowed to exceed their thermal capacities, the notions of risky voltage probability, *RVP*, and line flow overloading probability, *LFOP*, need to be introduced. For example, risk level can be used to determine the extent to which voltage rise/down and overloading could exist during a control cycle in the active network management systems (NMS). The risk-based NMS allows

investigating in detail the benefits and impacts of adopting different control cycles, quantifying in particular compliance of voltages with the EN50160 standard [55]. The proposed risk-based metrics evaluate the probability of voltage constraint violation and line flow overloading, respectively. Probability of voltage excursions and congestions can be controlled using a pre-defined risk level as given in [55]. These metrics can be defined mathematically as follows:

$$RVP_i(t, h) = \sum_s \rho_s \gamma_i(t, h) [BRVR_i^s(t, h) + BRVD_i^s(t, h)] \quad (28)$$

$$LFOP_{ij}(t, h) = \sum_s \rho_s BLFO_{ij}^s(t, h) \quad (29)$$

where

$$BRVR_i^s(t, h) = \begin{cases} 1 & ; \text{if } v_i^s(t, h) > v_{max,i} \\ 0 & ; \text{otherwise} \end{cases} \quad (30)$$

$$BRVD_i^s(t, h) = \begin{cases} 1 & ; \text{if } v_i^s(t, h) < v_{min,i} \\ 0 & ; \text{otherwise} \end{cases} \quad (31)$$

$$BLFO_{ij}^s(t, h) = \begin{cases} 1 & ; \text{if } l_{ij}^s(t, h) > l_{max,ij} \\ 0 & ; \text{otherwise} \end{cases} \quad (32)$$

If we want to formulate the previously mentioned ODGA as a risk-constrained convex model, the equivalent linear inequalities of (30), (31) and (32) should be defined as (33), (34) and (35), respectively.

$$v_i^s(t, h) - v_{max,i} > [BRVR_i^s(t, h) - 1] M \quad (33a)$$

$$v_i^s(t, h) - v_{max,i} < BRVR_i^s(t, h) M \quad (33b)$$

$$v_{min,i} - v_i^s(t, h) > [BRVD_i^s(t, h) - 1] M \quad (34a)$$

$$v_{min,i} - v_i^s(t, h) < BRVD_i^s(t, h) M \quad (34b)$$

$$l_{ij}^s(t, h) - l_{max,ij} > [BLFO_{ij}^s(t, h) - 1] M \quad (35a)$$

$$l_{ij}^s(t, h) - l_{max,ij} < BLFO_{ij}^s(t, h) M \quad (35b)$$

Here, the square of the magnitude of the voltage lower bound $v_{min,i}$ and upper bound $v_{max,i}$ are in per unit values, and $l_{max,ij}$ is the magnitude of the thermal capacity of line (i, j) in p.u.. Also, M is sufficiently a big number.

C. Expected Line Loss Reduction (ELLR) and Expected Line Loss Increment (ELLI)

Depending on the location, generation and load at a given instant, DG may unload lines and reduce losses or, alternatively may increase the losses. These indices express respectively, the expected energy loss reduction or increment for a given time horizon and mathematically are given as follows:

$$ELLR = \sum_{s \in \mathcal{S}} \rho_s \sum_{(i,j) \in \mathcal{E}} \sum_{t \in \mathcal{T}} \sum_{h \in \mathcal{H}} LR_{ij}^s(t, h) \quad (36)$$

$$ELLI = \sum_{s \in \mathcal{S}} \rho_s \sum_{(i,j) \in \mathcal{E}} \sum_{t \in \mathcal{T}} \sum_{h \in \mathcal{H}} LI_{ij}^s(t, h) \quad (37)$$

$$LR_{ij}^s(t, h) = BLLR_{ij}^s(t, h) [LL_{ij}^0(t, h) - LL_{ij}^s(t, h)] \quad (38)$$

$$LI_{ij}^s(t, h) = BLLI_{ij}^s(t, h) [LL_{ij}^s(t, h) - LL_{ij}^0(t, h)] \quad (39)$$

where

$$LL_{ij}^s(t, h) = r_{ij} l_{ij}^s(t, h). \quad (40)$$

Here $LL_{ij}^s(t, h)$ denotes the line-loss in scenario s , at line ij at day t and at hour h after DG addition. $LL_{ij}^0(t, h)$ denotes the line-loss at line ij at day t and at hour h before DG addition. LR and ELI define the amounts of line-loss reduction and increment with respect to the line-loss before DG installation, respectively. Binary variables $BLLR$ and $BLLI$ are used to count the line loss reduction and increment, respectively. If line loss with DG is lower than that of before DG employment, $BLLR$ will be equal to one, and will be zero, otherwise. In contrast, if the line loss with DG is greater than that of before DG employment, $BLLI$ will be equal to one, and zero, otherwise.

VI. NUMERICAL RESULTS

A. Test System Data

The performance of the proposed models is evaluated using IEEE 33-bus RDS. Detailed load and branch data of this test system are obtained from [56]. Base values of this system are 12.66 kV and 100 MVA.

With the consideration of the land space limit, it is also assumed that the maximum size of DG unit that can be installed at each node is 1500 kVA with discrete interval capacity of 100 kVA. The ampacity of conductors between nodes 1-2 and 2-3 are assumed to be 350 A, and the ampacity of other conductors is assumed to be 250 A. In case studies 1 and 2, the maximum DG penetration limit, λ , in the system is set at 50%. The square magnitudes of voltage lower and upper limits are set to be 0.9025 p.u. and 1.1025 p.u., respectively.

The hourly wind speed and solar irradiance data for the site under study have been utilized to generate a Rayleigh and Beta PDFs for each time segment, respectively. From the hourly load data for the system under study and the IEEE-RTS system [57], the load profile is assumed as a percentage of the annual peak load which can be found in [17]. **The DG units are assumed to operate at unity power factor and are considered as not having the capability to control voltages, and therefore, they has been modeled in power flow equations as a negative load, i.e., as a PQ node.**

For the study cases in Subsections *B* to *D*, nodes 14, 18 and 32 are considered as the candidate nodes and in Subsection *E* nodes 6,14,18,22,32 are assumed as candidate nodes for DG integration. The candidate buses can be selected according to some parameters such as investor decisions, availability of energy resources, land space, etc. When the candidate buses are determined, it is the utilities task to install their DGs in the candidate nodes or not. The utility will perform this task in a way to get the maximum benefits. Several scenarios are considered in the study which are listed below:

Scenario 1: base case (without DG)

Scenario 2: only wind DG unit (maximum 1500 kW at each candidate node)

Scenario 3: only PV DG unit (maximum 1500 kW at each candidate node)

Scenario 4: only Biomass DG unit (maximum 1500 kW at each candidate node)

Scenario 5: mix of wind, PV and Biomass DG units (maximum capacity of 500 kW for each type at each candidate bus)

TABLE III
RESULTS OF CONVEX MODELS TO SOLVE ODGA: OPTIMIZATION OBJECTIVES
AND COMPUTATION TIMES.

OPF model	energy loss minimization			voltage maximization		
	VI	ELI	Time(s)	VI	ELI	Time(s)
MISOCP	1.047	0.47	1024	1.073	0.607	1012
MIQP	1.046	0.51	8.0	1.064	0.594	4.0
MIQCP	1.055	0.46	86	1.070	0.600	103

TABLE IV
EFFECTS OF DG TYPES ON PERFORMANCE METRICS, FIXED SUBSTATION
VOLTAGE.

Metrics	Scen#2	Scen#3	Scen#4	Scen#5
VI	1.003	1.012	1.035	1.032
$IVRP$	0.935	0.948	1.0	1.0
ELI	0.92	0.79	0.51	0.512
$ELLR$ (MWh)	46.56	130.0	309.3	304.3
$ELLI$ (MWh)	0.00	6.525	10.23	6.97

Each single objective problem has been solved using the modeling language GAMS [58] and solver MOSEK on a computer with Pentium(R) Dual-Core CPU @ 2 GHz and 4 GB of RAM.

B. Comparison of solution methods

Here, the proposed multi-period OPF-based ODGA models were employed with the energy loss index minimization and voltage index maximization objectives as given in Table III. This study was implemented for Scenario 5 over the summer season (24 time periods). This table gives the objectives and computation times obtained by each model. The results of this case study show that all models found approximately the same solution results. The energy losses reduction of 49.1% is obtained by the MIQP, 52.7% by the MISOCP model and 53.3% by the MIQCP model. The computation time of the MISOCP model is the most while the MIQP model is the lowest. The MIQCP model has the computation time between them. It should be noted that, minimization of ELI and maximization of VI will enhance each other. For example, when the objective function is the minimization of ELI , the MISOCP, MIQP and MIQCP, respectively will present 4.7%, 4.6% and 5.2% voltage improvement with respect to the voltages before DG addition. On the other hands, about 40% reductions in the energy losses will be obtained by all methods when the objective is maximization of VI . Therefore, the MISOCP and MIQCP models can be more accurate than MIQP which neglects losses in its constraints, but significantly have longer computation time to solve using currently available algorithms.

C. Comparison between DG types

The effects of location and size of wind, PV and biomass DG units on the voltage profile and losses are evaluated via scenarios 1 to 5. We will show that besides these effects, the system performance will be affected by the DG energy production patterns. Obviously, line-loss reductions and voltage profile improvements are due to reductions in power flows resulting from the introduction of DG. All scenarios that include biomass DG are superior to other scenarios (including intermittent generation) from a loss-reduction and voltage

TABLE V
OPTIMAL MW SIZE (NUMBER) AND LOCATION OF DG FOR ENERGY LOSS
MINIMIZATION, FIXED SUBSTATION VOLTAGE.

DG type	Candidate bus	Scen#2	Scen#3	Scen#4	Scen#5
Wind	14	0.7(7)	-	-	-
	18	0.1(1)	-	-	-
	32	0.9(9)	-	-	0.5(5)
PV	14	-	0.8(8)	-	-
	18	-	0.2(2)	-	-
	32	-	1.2(12)	-	-
Bio.	14	-	-	0.4(4)	0.4(4)
	18	-	-	0.1(1)	0.1(1)
	32	-	-	0.6(6)	0.5(5)

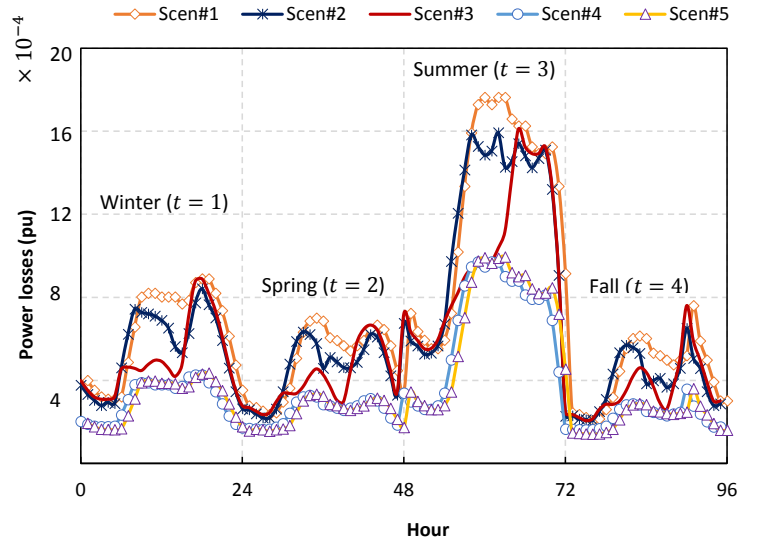


Fig. 1. Power losses for scenarios 1 to 5 while minimizing energy losses, fixed tap position.

improvement perspective, and biomass is the dominant renewable resource in these scenarios due to the firm output generation. This is due to the variability of wind power and PV generation and the limited reliance on power provision at moments where it could be beneficial particularly at peak demand. Among wind and PV DGs, the installed capacity of wind DG is lower than that of PV DG. The explanation is that installed capacity of wind DG restricted by voltage rise issue in the states of maximum generation and minimum load (as wind speed involve larger amounts of uncertainty). Despite wind turbine, PV DG is permitted to be installed more capacity (about 500 kW), while in most states maximum generations have been occurred at peak load demand; hence the improvement on performance indices will be higher than that of wind-based DG.

The results of ODGA for energy loss minimization for Scenarios 2-5 are shown in Tables IV and V, Fig. 1 and Fig. 2. These planning problems have been solved using MIQCP model. The results of Scenarios 2-5 show that the introduction of DG reduces the annual energy losses with respect to scenario 1. The values of ELI , $ELLR$ and $ELLI$ in Table IV indicate that wind based DG has the least contribution to energy losses reduction, about 10%, while biomass DG by 50% reduction is the most beneficial DG option. The energy loss reduction of Scenario 3 (only PV DG) is higher than that for

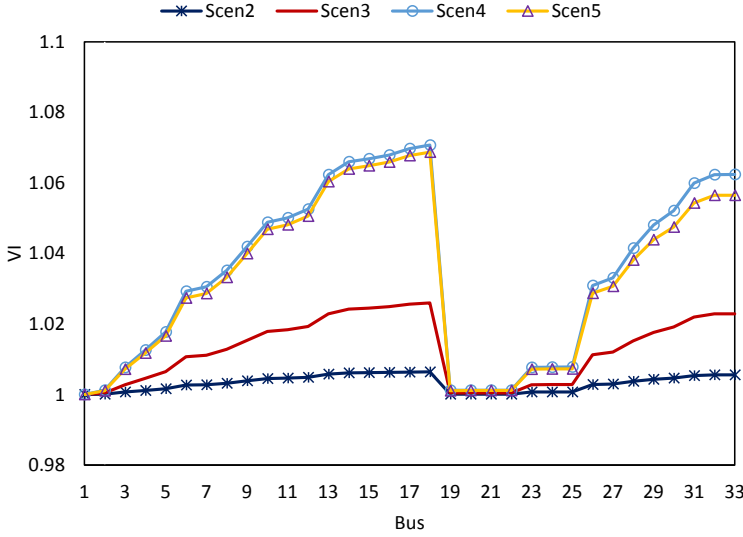


Fig. 2. Effects of DG types on VI while minimizing energy losses, fixed tap position.

Scenario 2 (only wind DG), however, there is large amounts of uncertainty in both wind speed and solar irradiance. The reason is that, the capacity of installed PV DG in Scenario 3 is 0.5 MW which is greater than the wind DG capacity in Scenario 2. Also, it is evident that *ELLR* increases as *ELI* decreases. *VI* and *IVRP* metrics are used to quantify the voltage profile improvement in a year and the results are given in the 2nd and 3rd rows of Tables IV. It can be seen that these metrics result the highest value for Scenarios 4 and 5, where the biomass DG units were considered due to its firm generation pattern. As seen from Table V, in all scenarios the simulation of ODGA placed and sized the highest DG unit at bus 32. Bus 14 is the second most preferred bus to install DG, and bus 18 is the least one. **Considering the case that the total power of three types is 1500 kW without restriction of each type, the results are similar to that of scenario 4.**

D. Optimal On-Load Tap-Changing (OLTC) adjustment

In this section, we assumed that substation transformers are equipped with OLTC capability. By implementing OLTC, more DG may be introduced in the system (see Tables VI and VII), as OLTC can change dynamically at the substation. This may change voltage profile and line losses. The effects of OLTC on energy loss minimization, for example, are evaluated in this part. The static model of OLTC is used to model the OLTC in the proposed planning problem. In this model, tap positions are considered as discrete variables. We consider the voltage magnitude at the substation bus, $V_1^s(t, h)$, as a decision variable with the following constraints:

$$V_1^s(t, h) = T_{min} + T_{tap} \sum_{n=1}^{N_{tap}} \eta_n^s(t, h) \quad (41)$$

$$v_1^s(t, h) = (V_1^s(t, h))^2. \quad (42)$$

The design of the transformers is in such a way that the tap ratio usually varies between 0.9 to 1.1 ($\pm 10\%$). T_{min} is the minimum voltage magnitude at the lowest tap position, N_{tap} is the number of all possible tap positions. η_n is a binary variable counting tap ratios. We set T_{min} at 0.9, $T_{tap} = 0.05$ and $N_{tap} = 4$ in this paper.

TABLE VI
EFFECTS OF DG TYPES AND OLTC OPERATION AT SUBSTATION BUS ON PERFORMANCE METRICS.

Metrics	Scen#2	Scen#3	Scen#4	Scen#5
<i>VI</i>	0.99	1.02	0.94	0.96
<i>IVRP</i>	0.422	0.748	0.122	0.243
<i>ELI</i>	0.902	0.80	0.51	0.512
<i>ELLR</i> (MWh)	60.5	132.33	309.3	304.8
<i>ELLI</i> (MWh)	1.24	10.52	10.23	7.412
%OLTC Operation	39.5	16.6	12.5	25

TABLE VII
OPTIMAL MW SIZE (NUMBER) AND LOCATION OF DG FOR ENERGY LOSS MINIMIZATION CONSIDERING OLTC AUTOMATIC OPERATION.

DG type	Candidate bus	Scen#2	Scen#3	Scen#4	Scen#5
Wind	14	1(10)	-	-	0.2(2)
	18	-	-	-	-
	32	1.5(15)	-	-	0.5(5)
PV	14	-	0.9(9)	-	-
	18	-	0.3(3)	-	-
	32	-	1.2(12)	-	-
Bio.	14	-	-	0.4(4)	0.4(4)
	18	-	-	0.1(1)	0.1(1)
	32	-	-	0.6(6)	0.5(5)

The measure of %OLTC operation is used in this paper to count the ratio of the number of hours in which a tap position changes over the number of total hours in a year.

VI and *IVRP* metrics are used to quantify the voltage profile improvement in a year and the results are given in the 2nd and 3rd rows of Table VI. It can be seen that these metrics result in the lowest value for Scenarios 4 and 5. *VI* in Scenario 2 is 0.99 which indicates that wind integration has had a negative impact on voltage profile, but the *IVRP* metric shows the probability of voltage improvement is 0.422. In Scenarios 4 and 5, where the biomass DG units were considered, the *VI* and *IVRP* reach the lowest values. The results of Scenario 4 and 5 show that biomass DG units are the most beneficial DG unit for energy loss minimization, whereas, its contribution to voltage improvement is the least with a *IVRP* and *VI* of 0.122 and 0.94 for Scenario 4, and 0.243 and 0.96 for Scenario 5, respectively. $VI = 1$ means that DG units will not impact on the voltage profile. While we can see from the second column of Table VI that the value of yearly *VI* couldn't individually represent the voltage profile variation due to the DG employment, as *IVRP* exhibits more than 40% the probability of interest voltage rise with the DG addition. The Scenarios including wind based DG units, i.e., Scenarios 2 and 5, indicate that due to the larger uncertainty of wind speed with respect to solar radiation, the percentage of OLTC operations during a year are superior to other Scenarios. Because of firm output generation of biomass DG units, the %OLTC operation in Scenario 4 is the lowest one.

E. Risk-constrained maximum DG penetration

The problem of risk-constrained maximum DG penetration is studied in this section. We will show that how the decision variables change with the change of proposed risks levels. This study proves that line overloading and voltage rises are the limiting factors that manifest themselves under different conditions. Four different cases

TABLE VIII
RESULTS OF RISK-CONSTRAINED MAXIMUM DG PENETRATION PROBLEM.

Metrics	Case1	Case2	Case3	Case4
λ	0.23	0.32	0.23	0.37
VI	1.084	1.09	1.086	1.02
$IVRP$	1.0	0.96	1.0	0.50
RVP	0.0	0.037	0.0	0.043
ELI	0.83	1.2	0.813	1.12
$ELLR$ (MWh)	120.6	111.5	135.4	106.9
$ELLI$ (MWh)	21.6	234.7	21.6	183.0
$LFOP$	0.0	0.0	0.0	0.001

are considered for determining maximum PV DG penetration in the test system. The problems of these cases are formulated as risk-constrained probabilistic optimization problems which have the form of MIQCP problem. The mathematical expression of this problem can be summarized as follows:

$$\text{maximize } \lambda \quad (43)$$

subject to

$$(6), (9) - (14), (22) - (25), (28), (29), (33), (34) \quad (44a)$$

$$\sum_{i \in \mathcal{N}} \sum_{t \in \mathcal{T}} \sum_{h \in \mathcal{H}} RVP_i(t, h) \leq \alpha \quad (44b)$$

$$\sum_{(i,j) \in \mathcal{E}} \sum_{t \in \mathcal{T}} \sum_{h \in \mathcal{H}} LFOP_{ij}(t, h) \leq \beta \quad (44c)$$

$$P_{ij}^s(t, h)^2 + Q_{ij}^s(t, h)^2 - LC_{max,ij}^2 > [BLFO_{ij}^s(t, h) - 1] M \quad (44d)$$

$$P_{ij}^s(t, h)^2 + Q_{ij}^s(t, h)^2 - LC_{max,ij}^2 < BLFO_{ij}^s(t, h) M \quad (44e)$$

where, α and β are the allowable risk levels of RVP and $LFOP$, respectively. Four sets of these risk levels are assumed in this section: Case1: $\alpha = \beta = 0$; Case2: $\alpha = 0.05$ and $\beta = 0$; Case3: $\alpha = 0$ and $\beta = 0.05$; Case4: $\alpha = 0.05$ and $\beta = 0.05$. Nodes 6, 14, 18, 22 and 32 are assumed as candidate buses. The maximum allowable PV capacity that could be installed at these buses is set at 3 MW. The results are shown in Tables VIII and IX. As seen from the second and fourth columns of Table VIII, Cases 1 and 3 reach the same results. This highlights situations in which voltage rise are more restrictive than line overloading, see the results of Cases 1-3. Also, no line overloading is occurred in Case 3, i.e., $LFOP = 0$. This situation highly depends on the magnitude of the substation voltage. In other words, if we increase the difference between substation voltage magnitude and maximum voltage limit, line overloading may be more restrictive constraint than voltage rise. Note that, VI index is not a reliable measure of voltage profile in a case in which the voltage magnitude is permitted to be violated i.e., in Cases 2 and 4. It is evident that if the voltage and line overloading violations are permitted, more PV DG could be installed with respect to Cases 1-3; see Table IX.

VII. CONCLUSION

In this paper, three new convex models are proposed for optimal and maximal penetration of different types of DGs into the RDS. The optimization problem seeks to find the maximum

TABLE IX
OPTIMUM MW SIZE (NUMBER) AND LOCATION OF PV DG OBTAINED BY RISK-CONSTRAINED MAXIMUM DG PENETRATION PROBLEM.

DG type	Candidate bus	Case1	Case2	Case3	Case4
PV	6	2.9(29)	0.9(9)	2.4(24)	3(30)
	14	-	-	0.5(5)	-
	18	-	-	-	-
	22	1.3(13)	3(30)	1.3(13)	3(30)
	32	0.7(7)	3(30)	0.7(7)	1.9(19)

DG penetration, the minimum energy losses and the maximum voltage profile, while tackling thermal and voltage issues as well as the effects of renewable DGs (such as wind-based DG, PV DG, and biomass DG) and load uncertainties. At first, the basic MINLP model of the optimization problem is extracted. Then, this problem is relaxed to different types of convex models that can utilize a powerful class of convex optimization algorithms. Different probabilistic-based performance metrics are introduced to evaluate the benefits and risks of DG employment on DS. The results show that the quadratic programming model is efficient and also obtains satisfactory solutions, demonstrating its practicality for ODGA in large RDS. The second-order cone model seems more reliable in obtaining good solutions, but computationally to be somewhat is expensive. The proposed planning techniques have been applied to different scenarios for the IEEE 33-bus RDS. The results reveal that implementing DG can reduce annual energy losses and improve voltage profile. The effects of scenarios including biomass DG on energy losses reduction and voltage improvement are significant, as this DG generates firm output power. However, by allowing the problem to set optimal tap position of OLTC at substation bus, more DG can be installed, but the voltage improvement will be reduced in comparison to ODGA with the fixed tap ratio. Finally, the problem of the risk constrained maximum DG penetration with the proposed risk measures is proposed and evaluated in the planning problem.

REFERENCES

- [1] C. Wang and M. H. Nehrir, "Analytical approaches for optimal placement of distributed generation sources in power systems," *IEEE Trans. on Power Syst.*, vol. 19, no. 4, pp. 2068–2076, 2004.
- [2] P. M. Costa and M. A. Matos, "Avoided losses on lv networks as a result of microgeneration," *Elec. Power Syst. Res.*, vol. 79, no. 4, pp. 629–634, 2009.
- [3] T. Gözel and M. H. Hocaoglu, "An analytical method for the sizing and siting of distributed generators in radial systems," *Elec. Power Syst. Res.*, vol. 79, no. 6, pp. 912–918, 2009.
- [4] S.-H. Lee and J.-W. Park, "Selection of optimal location and size of multiple distributed generations by using kalman filter algorithm," *IEEE Trans. on Power Syst.*, vol. 24, no. 3, pp. 1393–1400, 2009.
- [5] D. Q. Hung, N. Mithulananthan, and R. Bansal, "Analytical expressions for dg allocation in primary distribution networks," *IEEE Trans. on Energy Convers.*, vol. 25, no. 3, pp. 814–820, 2010.
- [6] D. Q. Hung and N. Mithulananthan, "Multiple distributed generator placement in primary distribution networks for loss reduction," *IEEE Trans. on Ind. Electron.*, vol. 60, no. 4, pp. 1700–1708, 2013.
- [7] M. Vatani, D. S. Alkaran, M. J. Sanjari, and G. B. Gharehpetian, "Multiple distributed generation units allocation in distribution network for loss reduction based on a combination of analytical and genetic algorithm methods," *IET Gener., Transm. & Distrib.*, vol. 10, no. 1, pp. 66–72, 2016.
- [8] A. Keane and M. O'Malley, "Optimal allocation of embedded generation on distribution networks," *IEEE Trans. on Power Syst.*, vol. 20, no. 3, pp. 1640–1646, 2005.
- [9] M. AlHajri, M. AlRashidi, and M. El-Hawary, "Improved sequential quadratic programming approach for optimal distribution generation deployments via stability and sensitivity analyses," *Elec. Power Compon. and Syst.*, vol. 38, no. 14, pp. 1595–1614, 2010.

- [10] P. N. Vovos and J. W. Bialek, "Direct incorporation of fault level constraints in optimal power flow as a tool for network capacity analysis," *IEEE Trans. on Power Syst.*, vol. 20, no. 4, pp. 2125–2134, 2005.
- [11] M. Esmaili, "Placement of minimum distributed generation units observing power losses and voltage stability with network constraints," *IET Generation, Transmission Distribution*, vol. 7, pp. 813–821, Aug 2013.
- [12] L. F. Ochoa, A. Padilha-Feltrin, and G. P. Harrison, "Time-series-based maximization of distributed wind power generation integration," *IEEE Trans. on Energy Convers.*, vol. 23, no. 3, pp. 968–974, 2008.
- [13] L. F. Ochoa, C. J. Dent, and G. P. Harrison, "Distribution network capacity assessment: Variable dg and active networks," *IEEE Trans. on Power Syst.*, vol. 25, no. 1, pp. 87–95, 2010.
- [14] A. Kumar and W. Gao, "Optimal distributed generation location using mixed integer non-linear programming in hybrid electricity markets," *IET Gener., Transm. & Distrib.*, vol. 4, no. 2, pp. 281–298, 2010.
- [15] S. Porkar, P. Poure, A. Abbaspour-Tehrani-fard, and S. Saadate, "Optimal allocation of distributed generation using a two-stage multi-objective mixed-integer-nonlinear programming," *Eur. Trans. on Electr. Power*, vol. 21, no. 1, pp. 1072–1087, 2011.
- [16] Y. M. Atwa and E. F. El-Saadany, "Probabilistic approach for optimal allocation of wind-based distributed generation in distribution systems," *IET Renew. Power Gener.*, vol. 5, no. 1, pp. 79–88, 2011.
- [17] Y. Atwa, E. El-Saadany, M. Salama, and R. Seethapathy, "Optimal renewable resources mix for distribution system energy loss minimization," *IEEE Trans. on Power Syst.*, vol. 25, no. 1, pp. 360–370, 2010.
- [18] R. Al Abri, E. F. El-Saadany, and Y. M. Atwa, "Optimal placement and sizing method to improve the voltage stability margin in a distribution system using distributed generation," *IEEE Trans. on Power Syst.*, vol. 28, no. 1, pp. 326–334, 2013.
- [19] N. Khalesi, N. Rezaei, and M.-R. Haghifam, "Dg allocation with application of dynamic programming for loss reduction and reliability improvement," *Int. J. of Electr. Power & Energy Syst.*, vol. 33, no. 2, pp. 288–295, 2011.
- [20] R. A. Jabr and B. Pal, "Ordinal optimisation approach for locating and sizing of distributed generation," *IET Gener., Transm. & Distrib.*, vol. 3, no. 8, pp. 713–723, 2009.
- [21] D. Singh and R. Misra, "Effect of load models in distributed generation planning," *IEEE Trans. on Power Syst.*, vol. 22, no. 4, pp. 2204–2212, 2007.
- [22] L. F. Ochoa, A. Padilha-Feltrin, and G. P. Harrison, "Evaluating distributed time-varying generation through a multiobjective index," *IEEE Trans. on Power Del.*, vol. 23, no. 2, pp. 1132–1138, 2008.
- [23] M. A. Akbari, J. Aghaei, M. Barani, M. Savaghebi, M. Shafie-khah, J. M. Guerrero, and J. P. S. Catalao, "New metrics for evaluating technical benefits and risks of DGs increasing penetration," *IEEE Trans. Smart Grid*, vol. 8, pp. 2890–2902, Feb 2017.
- [24]
- [25]
- [26] A. A. El-Ela, S. M. Allam, and M. Shatla, "Maximal optimal benefits of distributed generation using genetic algorithms," *Electric Power Syst. Res.*, vol. 80, no. 7, pp. 869–877, 2010.
- [27] C. Novoa and T. Jin, "Reliability centered planning for distributed generation considering wind power volatility," *Elec. Power Syst. Res.*, vol. 81, no. 8, pp. 1654–1661, 2011.
- [28] V. R. Pandi, H. Zeineldin, and W. Xiao, "Determining optimal location and size of distributed generation resources considering harmonic and protection coordination limits," *IEEE Trans. on Power Syst.*, vol. 28, no. 2, pp. 1245–1254, 2013.
- [29] L. Wang and C. Singh, "Reliability-constrained optimum placement of reclosers and distributed generators in distribution networks using an ant colony system algorithm," *IEEE Trans. on Syst., Man, and Cyber. C*, vol. 38, no. 6, pp. 757–764, 2008.
- [30] F. S. Abu-Mouti and M. El-Hawary, "Optimal distributed generation allocation and sizing in distribution systems via artificial bee colony algorithm," *IEEE Trans. on Power Del.*, vol. 26, no. 4, pp. 2090–2101, 2011.
- [31] L. Arya, A. Koshti, and S. Choube, "Distributed generation planning using differential evolution accounting voltage stability consideration," *Int. J. of Electr. Power & Energy Syst.*, vol. 42, no. 1, pp. 196–207, 2012.
- [32] R. S. Rao, K. Ravindra, K. Satish, and S. Narasimham, "Power loss minimization in distribution system using network reconfiguration in the presence of distributed generation," *IEEE Trans. on Power Syst.*, vol. 28, no. 1, pp. 317–325, 2013.
- [33] B. Banerjee and S. M. Islam, "Reliability based optimum location of distributed generation," *Int. J. of Electr. Power & Energy Syst.*, vol. 33, no. 8, pp. 1470–1478, 2011.
- [34] J. A. Taylor and F. S. Hover, "Convex models of distribution system reconfiguration," *IEEE Transactions on Power Systems*, vol. 27, pp. 1407–1413, Aug 2012.
- [35] R. A. Jabr, R. Singh, and B. C. Pal, "Minimum loss network reconfiguration using mixed-integer convex programming," *IEEE Transactions on Power Systems*, vol. 27, pp. 1106–1115, May 2012.
- [36] R. A. Jabr, "Radial distribution load flow using conic programming," *IEEE Transactions on Power Systems*, vol. 21, pp. 1458–1459, Aug 2006.
- [37] R. A. Jabr, "A conic quadratic format for the load flow equations of meshed networks," *IEEE Transactions on Power Systems*, vol. 22, pp. 2285–2286, Nov 2007.
- [38] R. A. Jabr, "Optimal power flow using an extended conic quadratic formulation," *IEEE Transactions on Power Systems*, vol. 23, pp. 1000–1008, Aug 2008.
- [39] Q. Peng, Y. Tang, and S. H. Low, "Feeder reconfiguration in distribution networks based on convex relaxation of opf," *IEEE Transactions on Power Systems*, vol. 30, pp. 1793–1804, July 2015.
- [40] "Ibm - mathematical programming: Linear programming, mixed-integer programming and quadratic programming - ibm cplex optimizer - software." [Online]. Available: <http://www-01.ibm.com/software/integration/optimization/cplex-optimizer/>.
- [41] "Gurobi optimizer 5.0 - state-of-the-art mathematical programming solver." [Online]. Available: <http://www.gurobi.com/>.
- [42] W. El-Khattam, Y. Hegazy, and M. Salama, "An integrated distributed generation optimization model for distribution system planning," *IEEE Trans. on Power Syst.*, vol. 20, no. 2, pp. 1158–1165, 2005.
- [43] R. K. Singh and S. Goswami, "Optimum allocation of distributed generations based on nodal pricing for profit, loss reduction, and voltage improvement including voltage rise issue," *Int. J. of Electr. Power & Energy Syst.*, vol. 32, no. 6, pp. 637–644, 2010.
- [44] L. F. Ochoa and G. P. Harrison, "Minimizing energy losses: Optimal accommodation and smart operation of renewable distributed generation," *IEEE Trans. on Power Syst.*, vol. 26, no. 1, pp. 198–205, 2011.
- [45] G. Koutroumpetzis and A. Safigianni, "Optimum allocation of the maximum possible distributed generation penetration in a distribution network," *Elec. Power Syst. Res.*, vol. 80, no. 12, pp. 1421–1427, 2010.
- [46] T. Niknam, M. Zare, and J. Aghaei, "Scenario-based multiobjective volt/var control in distribution networks including renewable energy sources," *IEEE Trans. Power Del.*, vol. 27, no. 4, pp. 2004–2019, Oct. 2012.
- [47] Z. Salameh, B. Borowy, and A. Amin, "Photovoltaic module-site matching based on the capacity factors," *IEEE Trans. Energy Convers.*, vol. 10, no. 2, pp. 326–332, Jun. 1995.
- [48] J. M. S. Pinheiro, C. R. R. Dornellas, M. T. Schilling, A. C. G. Melo, and J. C. O. Mello, "Probing the new IEEE reliability test system (RTS-96): HL-II assessment," *IEEE Trans. Power Syst.*, vol. 13, pp. 171–176, Feb 1998.
- [49] N. Growe-Kuska, H. Heitsch, and W. Romisch, "Scenario reduction and scenario tree construction for power management problems," in *Power Tech Conference Proceedings*, vol. 3, IEEE, 2003.
- [50] P. Chiradeja and R. Ramakumar, "An approach to quantify the technical benefits of distributed generation," *IEEE Transactions on Energy Conversion*, vol. 19, pp. 764–773, Dec 2004.
- [51] L. Liberti, "Introduction to global optimization," *Lecture of Ecole Polytechnique, Palaiseau F*, vol. 91128, p. 12, 2008.
- [52] S. B. M. S. Lobo, L. Vandenberghe and H. Lebret, "Applications of second-order cone programming," *Linear Algebra and Its Applications*, vol. 284, p. 193228, Nov. 1998.
- [53] S. Boyd and L. Vandenberghe, *Convex Optimization*. International series of monographs on physics, New York:Cambridge Univ. Press, 2004.
- [54] "The electricity supply, quality and continuity regulations 2002, uk department of trade and industry," 2002.
- [55] S. W. Alnaser and L. F. Ochoa, "Advanced network management systems: A risk-based ac opf approach," *IEEE Transactions on Power Systems*, vol. 30, pp. 409–418, Jan 2015.
- [56] M. E. Baran and F. F. Wu, "Network reconfiguration in distribution systems for loss reduction and load balancing," *IEEE Transactions on Power Delivery*, vol. 4, pp. 1401–1407, Apr 1989.
- [57] J. M. S. Pinheiro, C. R. R. Dornellas, M. T. Schilling, A. C. G. Melo, and J. C. O. Mello, "Probing the new IEEE reliability test system (rts-96): HI-II assessment," *IEEE Transactions on Power Systems*, vol. 13, pp. 171–176, Feb 1998.
- [58] B. A. McCarl, A. Meeraus, P. van der Eijk, M. Bussieck, S. Dirkse, P. Steacy, and F. Nelissen, "Mccarl gams user guide," 2014. [Available online]:<http://www.gams.com>.